ORIGINAL PAPER

Virtual screening of specific chemical compounds by exploring *E.coli* NAD$^+$-dependent DNA ligase as a target for antibacterial drug discovery

**Bashir Akhlaq Akhoon · Shishir K Gupta ·
Gagan Dhaliwal · Mugdha Srivastava ·
Shailendra K Gupta**

Abstract Unique substrate specificity compared with ATP-dependent human DNA ligases recommends *E.coli* NAD$^+$-ligases as potential targets. A plausible strategy is to identify the structural components of bacterial DNA ligase that interact with NAD$^+$ and then to isolate small molecules that recognize these components and thereby block the binding of NAD$^+$ to the ligase. This work describes a molecular modeling approach to detect the 3D structure of NAD$^+$-dependent DNA ligase in *E. coli* whose partial structure was determined by wet lab experiments and rest structure was left as such on the road for repairment. We applied protein-drug docking approach to detect the binding affinity of this enzyme with Quinacrine and some of its virtual derivatives. *In silico* docking results predict that the virtual derivative of Quinacrine (C21H26ClN3O2) has greater binding affinity than Quinacrine. Drug likeness value of 0.833 was observed for this derivative without showing any toxicity risk.

Keywords Computational drug discovery · DNA ligase · Drug target · NAD$^+$ · Quinacrine

B. A. Akhoon · G. Dhaliwal
Department of Bioinformatics,
Dolphin Post Graduate college of life Sciences,
Punjabi University,
Patiala 147002 Punjab, India

B. A. Akhoon (✉) · S. K Gupta · M. Srivastava
The Bioinformatica Solutions,
Society for Biological Research & Rural Development,
1/8, Vijay Khand, Gomti Nagar,
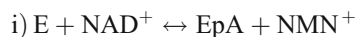Lucknow 226010 UP, India
e-mail: bashirakhlaq@gmail.com

S. K Gupta
Bioinformatics, Indian Institute of Toxicology Research (CSIR),
MG Marg, Lucknow, India 226001
e-mail: skgupta@iitr.res.in

Introduction

The discovery of *Escherichia coli* (NAD$^+$-dependent) and coliphage (ATP-dependent) DNA ligases, 40 years ago, was a watershed event in molecular biology [1–8]. NAD$^+$-DNA ligases have been suggested as possible targets for broad-spectrum antibacterial compounds [9–14] since they are indispensable for many fundamental processes in DNA metabolism including the linkage of Okazaki fragments during replication, recombination processes, and repair pathways requiring resynthesis of DNA [15, 16]. A requirement for an antibacterial enzyme target is that it should be essential for the organism and not present in the host. Currently, functional NAD$^+$-ligases have not been detected in humans, leading to speculation that they could be useful targets for broad-spectrum antibiotics [9–14, 17, 18]. NAD$^+$-ligase (LigA) is an essential enzyme in *E. coli* and it is likely that its homologous proteins are essential for all bacteria [19]. In general, bacterial NAD$^+$-ligases have sequences that are highly conserved and it is believed that such similarity carries through to their structure [15, 20] and this is one of the aspects in considering DNA ligase as a potential antibacterial target. DNA ligases are grouped into two families, ATP-dependent ligases and NAD$^+$-dependent ligases, according to the cofactor required for ligase-adenylate formation. It is the distribution of cofactor specificity that has led to the suggestion that NAD$^+$-dependent DNA ligases may be exploited as useful new targets for broad-spectrum antibacterial compounds [19–22]. Indeed, recent studies have begun to make important progress in identifying small molecules that have some specificity toward the inhibition of NAD$^+$-dependent DNA ligases [18, 23–26]. Apart from the difference in cofactor requirement, the reactions catalyzed by the two classes of DNA ligase are identical [16, 26]. The ATP-dependent DNA

ligases are found in all three-domain system of life (bacteria, archaea, and eukarya), whereas the NAD$^+$-dependent enzymes are present only in bacteria [19]. *Amsacta moorei* entomopoxvirus is the known exception where a eukaryotic virus codes for an NAD$^+$-dependent ligase [17]. At least one NAD$^+$- dependent DNA ligase (referred to as LigA) is found in every bacterial species and genetic studies have shown that the LigA gene is essential for the growth of *E. coli* [19]. All DNA ligases, prokaryotic as well as eukaryotic, catalyze the phosphodiester bond formation *via* three steps [27]: (1) adenylation of ligase, where the transfer of the AMP group from the cofactor to the active site lysine activates the enzyme, by hydrolysis of the pyrophosphate bond of NAD+ (or ATP) and the release of NMN (or pyrophosphate); (2) transfer of the AMP from ligase to the 5′-phosphate group at the single-strand DNA break site; and (3) DNA ligation with the release of free AMP. Whereas the last two steps of the DNA ligation are essentially the same for both eukaryotic and bacterial enzymes, the adenylation step differs substantially for the two classes of enzymes by virtue of their different cofactor requirements. In contrast to eukaryotic ligases, which use ATP as the cofactor, bacterial ligase uses NAD+ for the adenylation step.

Reaction catalysed:

i) $E + NAD^+ \leftrightarrow EpA + NMN^+$

ii) $EpA + pDNA \leftrightarrow AppDNA + E$

iii) $DNAOH + AppDNA \leftrightarrow DNApDNA + PA$

NAD$^+$-dependent DNA ligase is a multidomain protein [12] and [20]. It is composed of N-terminal adenylation domain followed by oligomer binding fold, zinc finger and helix-hairpin-helix motifs, and C-terminal BRCT (BRCA1 C-terminal) domain. The N-terminal adenylation domain containing the active site lysine is both necessary and sufficient to self-adenylate the enzyme [11, 28, 29].

The increasing incidence of drug-resistant bacterial infections has stimulated searches for new classes of antibacterial agents that work by novel mechanisms [30]. Many features of NAD$^+$-dependent DNA ligase make it an attractive target for antibacterial drug discovery. NAD$^+$-dependent ligases are present in all bacteria, essential for bacterial growth and are structurally conserved among bacteria but display unique substrate specificity compared with the ATP dependent ligases of humans and other mammals, therefore inhibitors of bacterial NAD$^+$-dependent DNA ligases are outstanding candidates for antibiotic development. Most of the discoveries concerning the function of domain 1a in *E. coli* LigA raise the prospects for identifying small molecules that either compete for the predicted NMN site on domain 1a (said site being absent from ATP ligases) or else interfere with the conformational

movements of domain 1a that are postulated to orchestrate the adenylate transfer reaction from NAD$^+$ [14]. In the course of a search for specific inhibitors, several representative of arylamino compounds have been identified that inhibit NAD$^+$-dependent ligases preferentially [31]. A common structural feature of the compounds that display specificity of action is the presence of an amino side chain (with four carbons separating the nitrogens) attached to a heterocyclic ring system. Quinoline compounds that lack the diamino side chain (i.e., quinine, cinchonidine), and a bisquinoline compound with no side chain, showed no measurable inhibitory activity against either type of DNA ligase [31]. These data indicate that a structure with four carbon atoms separating two nitrogens is the minimum inhibitory element and this particular inhibitory moiety can be presented on a variety of scaffolds without losing its capacity for specific inhibition of the eubacterial ligase. It was found that Quinacrine, which is a more potent DNA-binding agent than CQ (a known antimalarial and DNA-binding agent [32, 33] is a much more potent inhibitor of the *E. coli* DNA ligase than is CQ.

Materials and methods

NAD$^+$-dependent DNA ligase sequence of 671 amino acid residues (Gene id. 16130337) was retrieved from GenBank database available at NCBI (http://www.ncbi.nlm.nih.gov). Instability index including other physical and chemical parameters were predicted by using ProtParam (http://www.expasy.ch/). HHsearch program (http://toolkit.lmb.uni-muenchen.de/hhpred), based on the pairwise comparison of Hidden Markov Models (HMM) was used as a homology searching tool. HHsearch creates an HMM from the input alignment and uses it to search HMMs created from other protein databases including the PDB and SCOP databases. HHsearch showed 100% identity with 2OWO template but after checking the PDB summary of 2OWO template, we observed that only the structure of 1-586 amino acid residues was examined by x-ray crystallography and rest structure was left as such on the road, hence an attempt was made to find a suitable template protein for the modeling of the target protein. We introduced multi-template modeling protocol and the template proteins were searched through HHsearch. From the homology search two templates, i.e., 2OWOA and 1I7bA were selected and were subjected to the Geno3D [34] that performs comparative protein structure modeling by spatial restraints (distances and dihedral) satisfaction. The model obtained was subjected to a series of tests for validation of consistency and reliability of the model using Procheck software. Among the three models generated by Geno3D, model2 was selected on the basis of core value and number of bad contacts as
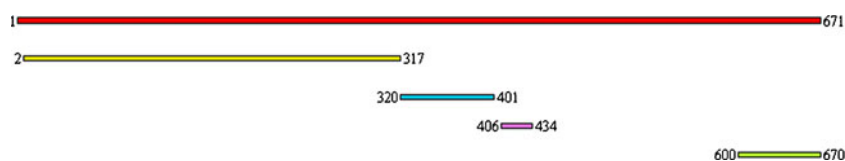
Fig. 1 Graphical representation of domain analysis. Query Sequence (1-671), Adenylation Domain (2-317), OB Fold Domain (320–401), Zinc Finger Domain (406–434), BRCT Domain (600–670)

evaluated by Procheck software. Model2 was prepared for docking by using WHAT IF server [35]. The prepared pdb file was once again evaluated by Procheck and it was found that the amino acid residues in disallowed region were moved to allowed regions but the number of bad contacts increased significantly. To get rid of this problem, Model2 was solvated and subjected to constraint energy minimization with a harmonic constraint of 100 kJ mol^{-1} Å^{-2} applied for all protein atoms, using the steepest descent and conjugate gradient technique to eliminate bad contacts between protein atoms and structural water molecules. Computations were carried out *in vacuo* with the GROMOS96 43B1 [36] parameters set, implementation of Swiss-PdbViewer and the refined model was once again evaluated by Procheck. After result analysis it was found that no amino acid residues were in generic and disallowed regions and also no bad contacts were observed. Hence the model2 was used for docking purpose.

Ligsite^{CSC} webserver (www.scoppi.biotech.tu-dresden.de/pocket/) was used to search the best pockets of the model2 for the identification of active site. Ligsite uses grids to detect functional sites, further; conally surfaces and degree of conservation are used for refinement. Grid points, which are at least a part of five surface-solvent-surface events are marked as a pocket [37]. Different pockets of the receptor were obtained and arranged according to their volumes. The pocket having the maximum surface area was selected and the nearest atom to the pocket was determined using the distance tool in Swiss PDB viewer.

2D structures of various virtual derivatives of Quinacrine (Pubchem id. 237) were obtained from Pubchem compound available at NCBI and their conversion to 3D structures was done by OpenBabel software. Some PDB files derived from 2D SDF files contain H_2O molecules, Cl, HCl, CH_4 *etc.* impurities which need to be removed before docking and this operation

was done by Chem3D Ultra software. These virtual derivatives including Quinacrine were docked with the active site of the Model2 by using AutoDock4 software package [38].

Pharmacological properties of this virtual derivative as desired for a drug molecule were predicted by Molinspiration (http://www.molinspiration.com/cgi-bin/properties). Possible side effects and toxicity was checked by Osiris Property Explorer and PASS software. The Toxicity Prediction (TOPKAT) protocol of Accelrys Discovery Studio 2.0 was used to predict the ADMET - Hepatotoxicity. TOPKAT computes and validates assessments of the toxic and environmental effects of chemicals solely from their molecular structure by employing robust and cross-validated Quantitative Structure Toxicity Relationship (QSTR) models for assessing various measures of toxicity. Finally drug score was also confirmed by PASS.

Results

Primary sequence analysis

The sequence was found to contain an instability index of 36.13 which reveals that protein sequence will be stable in nature. Estimated half-life of 30 hours in mammalian reticulocytes (*in vitro*), >20 hours (yeast, *in vivo*) and >10 hours (Escherichia coli, *in vivo*) was predicted by Protparam tool.

Table 1 Procheck evaluation of the three models produced by Geno3D

Values	Model1	Model2	Model3
Core	76.3%	77.5%	75.1%
Allowed	19.0%	18.2%	20.1%
Generic	3.3%	1.9%	2.7%
Disallowed	1.4%	2.1%	2.1%
Bad contacts	2.0%	0.0%	1.0%

Table 2 Prockeck results

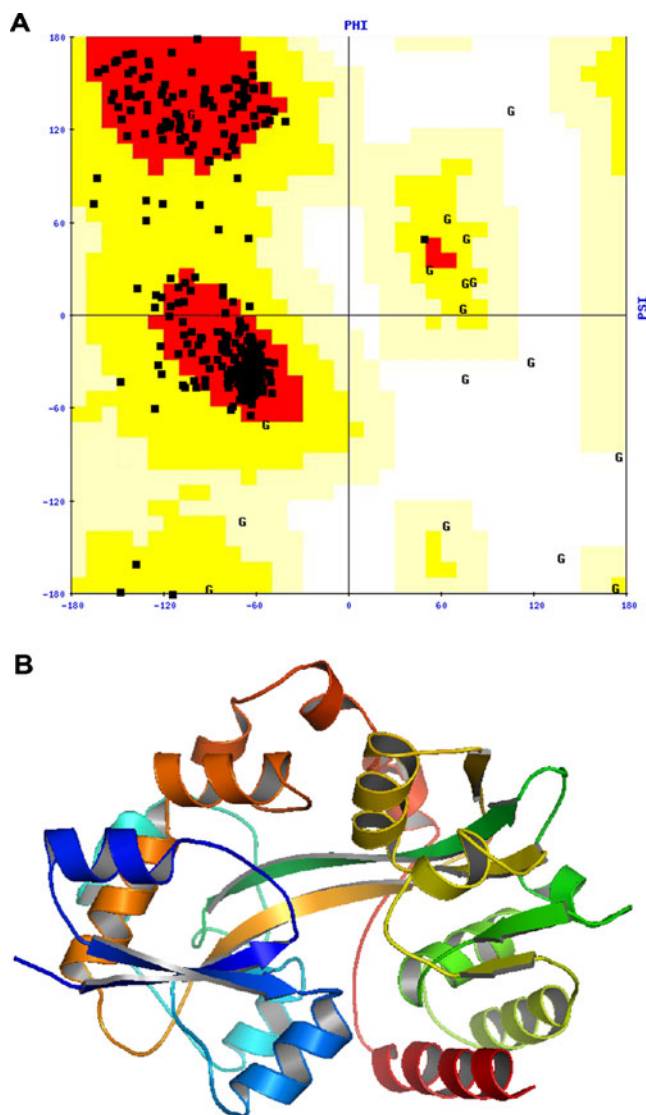| (A) Model2 after correction by What If server	
Values	Model2(a)
Core	88.5%
Allowed	10.8%
Generic	0.7%
Disallowed	0.0%
Bad contacts	9.0%
(B) Model2 after energy minimization	
Values	Model2(b)
Core	89.6%
Allowed	10.4%
Generic	0.0%
Disallowed	0.0%
Bad contacts	0.0%

Fig. 2 Best model (Model2) selected for docking after energy minimization. (**a**) Ramachandran plot of energy minimized model. (**b**) Best model (Model2) selected for docking after energy minimization

Domain analysis

Domain composition by CD search of NCBI is summarize in Fig. 1. In this figure the Adenylation Domain (2-317), OB Fold Domain (320–401), Zinc Finger Domain (406–434), and BRCT Domain (600–670) are shown.

Homology results

The alignment of protein sequences as generated by HHsearch explored that Protein data bank entry of 2OWOA and 1I7bA can be used as templates for comparative modeling of the query sequence. HHsearch showed, with a 100% probability, that 2OWO template can be used as best template as it showed 100% identity with the query sequence (E-value = 0) and hence was selected as one of the two best used templates. For the rest of the sequence it was revealed by homology search that with a probability of 99.69%, 1I7b might be used as a second best template for multitemplate modeling protocol as the predicted identity score of 47% with an E-value of 1.5e-17 was identified.

Comparative modeling and its validation

Three 3-D models of our query sequence were generated by Geno3D. In order to select the best model, we checked the structural validity of the models by Procheck program and the values are summarized in Table 1. Among the three models, model2 was selected on the basis of core value and bad contacts. Model2 was optimized by What If and the corrected model was once again evaluated by Procheck, further it was observed that besides increase in core value the bad contacts also get enhanced (Table 2a). Energy minimization of Model2 by Gromos96 was done to relieve the model from bad contacts and the evaluation of the energy minimized model in Table 2b showed that besides removal of bad contacts, all the amino acid residues in the

Table 3 Potential ligand binding sites in Model2 using a probe of radius 5.0 Å by Ligsite^{csc}

Atom no: 79,80,81,82,83,84,85,86,87,88,115,116,492,507,509,532,533,534,725,726,732,735,736,737,738,737, 738,1634,1635,1636,1637,1638,1639,1640,1835,1837,1838,1839,1847,1853,1854,1855,2378,2379,2380,2381,2382,2383,2384, 2407,2408,2410,2416,2417,2418,2419,2420,2432,2435,2436.

Atom name: CB, CG, CD1, CD2, NE1, CE2, CE3, CZ2, CZ3, CH2, CZ, OH, O, CD1, CE1, CB, CG, CD, C, O, CA, CB, CG, SD, CE, CD2, NE1, CE2, CE3, CZ2, CZ3,CH2, CE2, CZ2, CZ3, CH2, CE, CG, OD1, OD2, CD2, NE1, CE2, CE3, CZ2, CZ3, CH2, CG, OD1, N, CG2, N, CA, C, O, CA, CB, OG.

Amino acid residue: TRP, TRP, TRP, TRP, TRP, TRP, TRP, TRP, TRP, TRP, TRP, TRP, TRP, TRP, LYS, LYS, LYS, ASP, ASP, MET, MET, MET, MET, MET, TRP, TRP, TRP, TRP, TRP, TRP, TRP, TRP, TRP, TRP, TRP, MET, ASP, ASP, ASP, TRP, TRP, TRP, TRP, TRP, TRP, TRP, ASP, ASP, VAL, VAL, GLY, GLY, GLY, GLY, SER, SER, SER.

Chain: A Residue no: 34, 34, 34, 34, 34, 34, 34, 34, 34, 37, 37, 85, 86, 86, 89, 89, 89, 113, 113, 114, 114, 114, 114, 114, 229, 229, 229, 229, 229, 229, 229, 229, 255, 255, 255, 255, 256, 257, 257, 257, 326, 326, 326, 326, 326, 326, 326, 329, 329, 330, 330, 331, 331, 331, 331, 334, 334, 334.

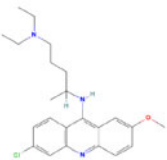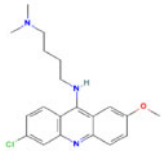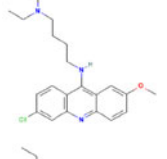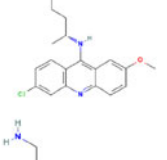**Table 4** Chemical structure of Quinacrine derivatives and their docked energy
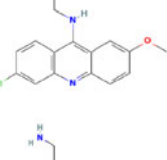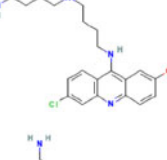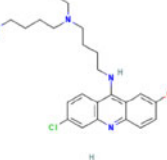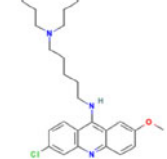
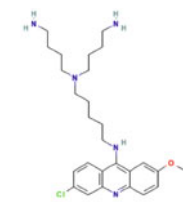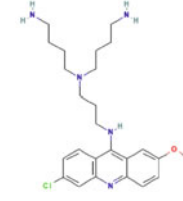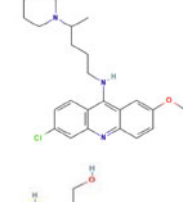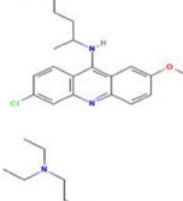| Chemical Id	Structure	Docked energy (Kcal/mol)
237 (Quinacrine)		-7.64
410993		-10.19
22709		-10.32
446536		-10.17
511165		-9.58
470841		-7.95
470842		-10.37
470843		-9.08

Table 4 (continued)
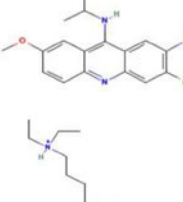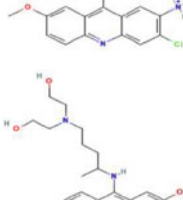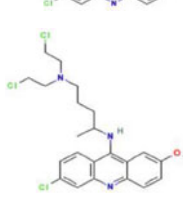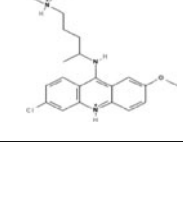
470844		-10.73
470838		-8.38
222130		-8.34
18331032		-12.56
3122093		-11.14
4995522		-11.37
12207957		-9.94
24180972		-11.48
15329120		-11.39

Fig. 3 Graphical representation of AutoDock results
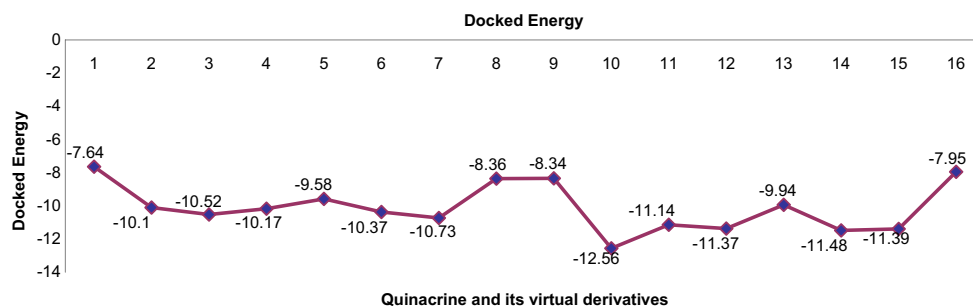
generic and disallowed regions were removed and added to core and allowed regions, hence made it the best model for docking purpose. The Ramachandran plot analysis of the model prepared for docking is shown in Fig. 2a and its 3D structure is depicted in Fig. 2b.

Ligand binding sites

Among the three pockets displayed by Ligsite^{csc}, pocket3 was selected as the best pocket because the distance of the Lys89 residue from pocket3 was very small as compared to other pockets. DNA ligases catalyze the joining of ends of nicked double-stranded DNA by a process that involve adenylation of a critical lysine residue within the active site and after checking the domains of the sequence by using CD search of NCBI, it was confirmed that Lys89 residue lies in the adenylation domain, hence Lys89 was selected as the active site residue. All potential ligand binding sites in Model2 using a probe of radius 5.0 Å by Ligsite^{csc} is illustrated in Table 3.

Docking results

Docking analysis was performed by Autodock4 and after scoring of docking results, it was observed that virtual derivative of Quinacrine with Pubchem ID 18331032 showed greater binding affinity with NAD$^+$-dependent DNA ligase in *E.coli* than Quinacrine. The chemical structure of quinacrine and its various derivatives with their docked energy is shown in Table 4. The best docked Quinacrine derivative is visualized in Fig. 3 while various energies calculated by Autodock4 software and the variables are illustrated in Table 5 and shown graphically in Fig. 4. Comparative structures of Quinacrine and its best known derivative are shown in Fig. 5 to get insight into their structural variation.

Drug likeness and toxicity risk check

Molinspiration result of Quinacrine derivative with Pubchem compound Id 18331032 is illustrated in Table 6. Osiris Property Explorer indicates that there are no toxicity risks

Table 5 Various energies calculated by Autodock4 software

| Inhibitor id	Binding	Intermol	Total Internal	Unbound	Vdw-hb-dessolvation	Electrostatic
237	-7.64	-9.56	0.0	0.0	-9.7	0.14
410933	-10.19	-12.24	81.91	81.91	-12.24	0.06
22709	-10.32	-13.11	82.24	81.91	-13.04	-0.07
446536	-10.17	-12.09	0.0	0.0	-8.8	-3.29
511165	-9.58	-11.7	82.28	82.08	11.74	0.04
470842	-10.37	-13.22	4.66	0.0	0.0	-0.44
470843	-9.08	-12.06	-1.5	0.18	-12.05	0.0
470844	-10.73	-15.44	-1.02	-0.79	-15.18	-0.26
470838	-8.38	-13.24	1.88	1.41	-13.2	0.04
222130	-8.34	-9.82	81.49	81.92	-9.85	0.03
18331032	-12.56	-15.34	0.1	0.07	-15.38	0.05
3122093	-11.14	-13.34	0.02	0.02	-13.43	0.09
4995522	-11.37	-14.02	1.79	0.79	-10.11	-3.9
12207957	-9.94	-13.52	0.2	0.14	-13.86	0.33
24180972	-11.48	-13.4	1.92	0.0	0.04	0.0
15329120	-11.39	-13.04	0.72	0.72	-10.66	-2.37
470841	-7.95	-13.27	1.13	0.2	-13.27	0.0
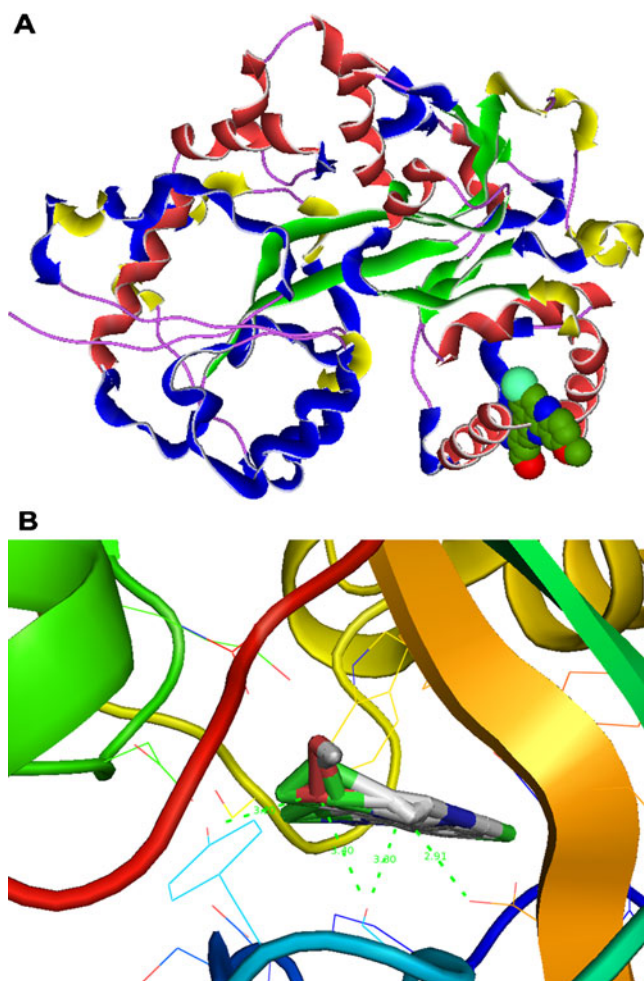
Fig. 4 Visualization and surface representation of Quinacrine derivative (C21H26ClN3O2) docked into active site of NAD⁺-dependent DNA ligase. (a) Visualization of the best docking by using Hex software. Helix (Red), Beta Sheet (Green), Turns (Blue), 310 helix (Yellow), Loops (Purple), Ligand -18331032 (CPK). (b) Surface representation of the NAD+-Dependent DNA ligase in E.coli and Quinacrine derivative with Pubchem Id 18331032 by Pymol visualizer
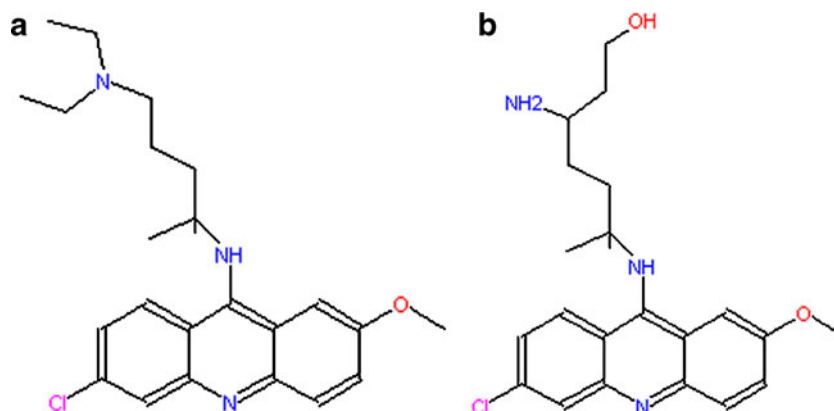
like mutagenic, tumorigenic, irritant and reproductive effects. PASS software evaluation (Pa>Pi) also confirmed that there are no possible side effects and toxicity of this compound. The hepatotoxicity score as predicted by Accelrys Discovery Studio 2.0 is the sum of the predicted values (0 and 1) from all individual trees that comprise the ensemble recursive partitioning model, divided by the total number of trees in that model. The closer the hepatotoxicity scores are to either 0 or 1, the more closely the predictions agree with each other. Compounds with scores distant from 0.5 tend to be predicted correctly more frequent than molecules with scores close to 0.5. Confidence level of 0 score value was observed for the newly predicted best derivative of Quinacrine which confirmed that this ligand will be non-hepatotoxin in nature. Drug-likeness value of 0.833 was observed for this relative molecule of Quinacrine by PASS.

Additional information

It was observed by PASS software (Pa>0.100) that besides acting as an antibacterial drug, this molecule can also have possible molecular mechanisms like Neuropeptide Y antagonist, Potassium channel activator and nitric oxide agonist with possible pharmacological effects like uric acid excretion stimulant, diuretic and vasodilator.

Discussion

Multiple drug resistance among bacterial pathogens is spreading even in developed countries and has made many currently available antibiotics ineffective. As a consequence the number of reports on therapy failures increases and treatment costs rise, causing a growing public health problem. Thus, the search for novel antibacterial classes with innovative mechanisms of action is crucial to keep pace with the innate adaptability of the bacterial population. The high degree of conservation of Eubacterial DNA ligases and their cofactor specificity have lead to the

Fig. 5 Comparative structure of Quinacrine and its virtual derivative (C21H26ClN3O2). (a) Quinacrine. (b) Quinacrine derivative with PubChem compound Id 18331032

Table 6 Molinspiration result of Quinacrine derivative with Pubchem compound Id 18331032

MiLogP	TPSA	natoms	MW	Non	nOHNH	nviolations	nrotb	volume
4.283	356.085	80.404	27	387.911	5	4	0	8

assumption that these enzymes may be a potential target for new bactericidal drugs. The drug-binding sites of ligA are ideally unique and conserved among NAD^+-DNA ligases. The three-dimensional (3D) structure details of proteins are of major importance in providing insights into their molecular functions. Further analysis of 3D structures will help in the identification of binding sites and may lead to the designing of new drugs. In the present work, comparative modeling protocol was used for the prediction of the 3D structure of *E.coli* NAD^+ dependent DNA ligase. By comparing the template protein, a rough model was constructed for the target protein. The rough model constructed was solvated and subjected to constraint energy minimization with a harmonic constraint of 100 kJ mol^{-1} Å^{-2} applied for all protein atoms, using the steepest descent and conjugate gradient technique to eliminate bad contacts between protein atoms and structural water molecules. As the N-terminal adenylation domain containing the active site lysine is both necessary and sufficient to self-adenylate the enzyme [11, 28, 29], the refined model was explored for the identification of the best binding pocket and the results predicted in this study were in consistent with the experimental studies that have been already approved.

Discovery of novel lead compounds through virtual screening (VS) of chemical databases against protein structures is an emerging and promising step in computer-aided drug design [39–42]. The development of an efficient bactericidal drug can essentially gain from the deciphering of the structural components of NAD^+ ligases interacting specifically with NAD^+. Given the structure of a target protein active site and a potential small ligand, VS predicts the binding mode and the binding affinity for each ligand and ranks a series of candidate ligands. Drugs that discriminate between DNA ligases from different sources may have antieubacterial activity. A group of arylamino compounds are specific inhibitors of eubacterial DNA ligases. The arylamino compounds have been identified to interfere specifically with the NAD^+-dependent DNA ligase by interacting with residues that lie adjacent to the adenylation site. A diamino side chain (NCCCCN) is necessary for the specific inhibitory activity of arylamino compounds but this moiety can be presented on either a quinoline or an acridine nucleus. The DNA-binding ability of the ring system, to which the diamino side chain is attached, appears to enhance the potency of an inhibitor but is not a critical determinant of its specificity [31]. Aminoquinolines like Quinacrine could be modified to enhance uptake and the modified molecules ideally would have

potential as bactericidal drugs. Structure of 17 newly proposed compounds derived from the structural modifications of the Quinacrine was drawn and the alteration was limited to such an extent that the specific inhibitory action should not blocked but only the binding affinity should be enhanced. Free binding energy was estimated using the empirical scoring function included in AutoDock. The scoring function included the van der Waals interaction represented as a Lennard-Jones 6–12 dispersion/repulsion term, the hydrogen bonding represented as a directional 12–10 term, and the Coulombic electrostatic potential. The reasonable observed difference in binding energies and binding modes of various compounds with NAD^+ ligase was firmly associated with their varied chemical structure. It was observed that the virtual derivative of Quinacrine (C21H26ClN3O2) can act as a best alternative drug of Quinacrine. Further druglikeness and toxicity check also paved its way for *in vivo* studies to be used as anti bacterial drug for the prevention of a wide range of bacterial diseases.

Conclusions

Conformational changes in drug molecule affects the binding affinity of drugs with its potential target. Candidate ligands screened for binding to the conserved and functionally important surface of adenylation domain of bacterial ligaseA using AutoDock4 software showed that the virtual derivative of the Quinacrine with PubChem compound ID of 18331032 has greater binding affinity toward DNA ligase. Drug likeness as predicted by PASS software confirmed that this virtual derivative can act as a drug. Absence of side effects and toxicity risks as prevailed by Osiris Property Explorer and PASS software enhance the prospect that this ligand can be sent for clinical trials for *in vivo* studies so that this virtual ligand can be used as a best antibacterial drug in the future.

References

1. Gellert M (1967) Proc Natl Acad Sci USA 57:148–155
2. Olivera BM, Lehman IR (1967) Proc Natl Acad Sci USA 57:1426–1433
3. Olivera BM, Lehman IR (1967) Proc Natl Acad Sci USA 57:1700–1704
4. Weiss B, Richardson CC (1967) Proc Natl Acad Sci USA 57:1021–1028
5. Weiss B, Richardson CC (1967) J Biol Chem 242:4270–4278
6. Gefter ML, Becker A, Hurwitz J (1967) Proc Natl Acad Sci USA 58:240–247

7. Zimmerman SB, Little JW, Oshinsky CK, Gellert M (1967) Proc Natl Acad Sci USA 57:1841–1848
8. Becker A, Lyn G, Gefter M, Hurwitz J (1967) Proc Natl Acad Sci USA 58:1996–2003
9. Georlette D, Blaise V, Dohmen C, Bouillenne F, Damien B, Depiereux E, Gerday C, Uversky VN, Feller G (2003) J Biol Chem 278:49945–49953
10. Gong C, Martins A, Bongiorno P, Glickman M, Shuman S (2004) J Biol Chem 279:20594–20606
11. Kaczmarek FS, Zaniewski RP, Gootz TD, Danley DE, Mansour MN, Griffor M, Kamath AV, Cronan M, Mueller J, Sun D, Martin PK, Benton B, McDowell L, Biek D, Schmid MB (2001) J Bacteriol 183:3016–3024
12. Lee JY, Chang C, Song HK, Moon J, Yang JK, Kim HK, Kwon ST, Suh SW (2000) EMBO J 19:1119–1129
13. Singleton MR, Hakansson K, Timson DJ, Wigley DB (1999) Structure 7:35–42
14. Sriskanda V, Shuman S (2002) J Biol Chem 277:9695–9700
15. Timson DJ, Singleton MR, Wigley DB (2000) Mutation Res 460:301–318
16. Lehman IR (1974) Science 186:790–797
17. Sriskanda V, Moyer RW, Shuman S (2001) J Biol Chem 276:36100–36109
18. Brotz-Oesterhelt H, Knezevic I, Bartel S, Lampe T, Warnecke-Eberz U, Ziegelbauer K, Habich D, Labischinski H (2003) J Biol Chem 278:39435–39442
19. Wilkinson A, Day J, Bowater R (2001) Mol Microbiol 40:1241–1248
20. Doherty AJ, Suh SW (2000) Nucleic Acids Res 28:4051–4058
21. Shuman S, Lima CD (2004) Curr Opinion Struct Biol 14:757–764
22. Tomkinson AE, Vijayakumar S, Pascal JM, Ellenberger T (2006) Chem Rev 106:687–699
23. Srivastava SK, Dube D, Vandna K, Jha AK, Hajela K, Ramachandran R (2007) Proteins 69:97–111
24. Srivastava SK, Dube D, Tewari N, Dwivedi N, Tripathi RP, Ramachandran R (2005) Nucleic Acids Res 33:7090–7101
25. Srivastava SK, Tripathi RP, Ramachandran R (2005) J Biol Chem 280:30273–30281
26. Tomkinson AE, Levin DS (1997) BioEssays 19:893–901
27. Engler MJ, Richardson CC (1982) Academic Press, Inc New York 15:3–29
28. Timson DJ, Wigley DB (1999) J Mol Biol 285:73–83
29. Lim JH, Choi J, Kim W, Ahn BY, Han YS (2001) Arch Biochem Biophys 388:253–260
30. Miesel L, Greene J, Black TA (2003) Nat Rev Genet 4:442–456
31. Ciarrocchi G, MacPhee DG, Deady LW, Tilley L (1999) Animicrobial agents Chemother 43:2766–2772
32. Cohen SN, Yielding KL (1965) J Biol Chem 240:3123–3131
33. Scaria PV, Craig JC, Shafer RH (1993) Biopolymers 33:887–895
34. Combet C, Jambon M, Deléage G, Geourjon C (2002) Bioinformatics 18:213–214
35. Vriend GJ (1990) Mol Graph 8:52–56
36. Scott WRP, Hünenberger PH, Tironi IG, Mark AE, Billeter SR, Fennen J, Torda AE, Huber T, Krüger P, Gunsteren WF (1999) J Phys Chem A 103:3596–3607
37. Huang B, Schroeder M (2006) BMC Struct Biol 6:19
38. Morris GM, Goodsell DS, Halliday RS, Huey R, Hart WE, Belew RK, Olson AJ (1998) J Comput Chem 19:1639–1662
39. Doman TN, McGovern SL, Witherbee BJ, Kasten TP, Kurumbail R, Stallings WC, Connolly DT, Schoichet BK (2002) J Med Chem 45:2213–2221
40. Lyne PD (2002) Drug Discov Today 7:1047–1055
41. Shoichet BK, McGovern SL, Wei B, Irwin J (2002) Curr Opin Chem Biol 6:439–446
42. Shoichet BK (2004) Nature 432:862–865